PCCP

PAPER

View Article Online
View Journal | View Issue

Cite this: *Phys. Chem. Chem. Phys.*, 2022, **24**, 25816

A combined DFT-predictive and experimental exploration of the sensitivity towards nucleofuge variation in zwitterionic intermediates relating to mechanistic models for unimolecular chemical generation and trapping of free C_2 and alternative bimolecular pathways involving no free C_2†

Henry S. Rzepa, *[a] Miki Arita,[b] Kazunori Miyamoto *[b] and Masanobu Uchiyama *[bc]

Received 13th March 2022,
Accepted 8th October 2022

DOI: 10.1039/d2cp01214f

rsc.li/pccp

Following the recent report of the chemical generation and trapping at room temperatures of C_2, generated from an alkynyl phenyl iodonium salt, a computational analysis had indicated that both unimolecular fragmentation and bimolecular substitution mechanisms for the process could be envisaged. Here a combined theoretical and experimental analysis explores how the energetics of these mechanisms and resulting experimental products respond to variation in the nucleofuge. When the phenyl iodonium nucleofuge is replaced by pyridinium, trapping products are again obtained, which we conclude favours a bimolecular mechanism involving no free C_2. Trapped products in greater yield were also observed using dibenzothiophenium as the nucleofuge in both condensed solution phase and most significantly in a two-flask room temperature experiment in which a volatile species, presumed to be C_2, is transferred and trapped in a second flask. The energetics of the unimolecular fragmentation process producing C_2 are predicted to be too high to correspond to a facile thermal reaction, which means that an experimental/theoretical dichotomy remains to be explained.

Introduction

The long history[1] of the diatomic species C_2, of recent interest because of the intense debates about its bond order (2,3 or 4)[2] took a new turn recently regarding its reactivity, with the report of room temperature generation and trapping of this species by chemical means.[3,4] The reaction was thought to proceed at ambient or low temperatures from the transient zwitterionic intermediate **2** (X = IPh), itself formed by treating precursor **1** with a source of fluoride anion. The proposed mechanism involved unimolecular fragmentation of **2** to produce X = iodobenzene and **3** (free singlet state C_2, Fig. 1), followed by its trapping in solution using either 9,10-dihydroanthracene **7** or galvinoxyl radical and resulting in isolation of products **5**/**4** and from which participation of free C_2 was inferred (Fig. 2).[3,4] Scrambling of ^{13}C label in product **4a** (Fig. 2, $C_\alpha : C_\beta$ = *ca.* 8 : 2–1 : 1) also supported this conclusion.[3]

A commentary on this report[5,6] observed that the computed thermodynamics of this reaction using three different estimates indicated that the production of free C_2 and X = iodobenzene (path 1, Fig. 1) was likely to be highly endoenergic, in the range of +(43–53) kcal mol^{-1} and therefore that room

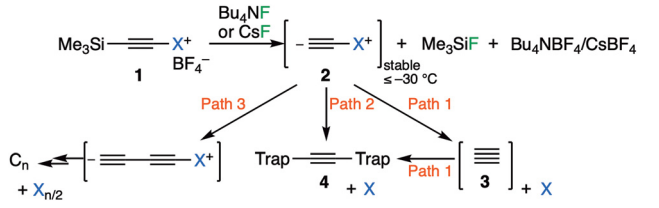

Fig. 1 Reaction scheme for proposed[3,4] chemical synthesis of singlet free C_2 **3** with alternatives. Path 1: unimolecular fragmentation followed by bimolecular trapping. Path 2: bimolecular trapping by 1,1- or 1,2-substitution. Path 3: bimolecular dimerisation *via* 1,1- or 1,2-substitution.

[a] *Department of Chemistry, Molecular Sciences Research Hub, Imperial College London, White City Campus, Wood Lane, London W12 OBZ, UK. E-mail: rzepa@imperial.ac.uk*
[b] *Graduate School of Pharmaceutical Sciences, The University of Tokyo, 7-3-1 Hongo, Bunkyo-ku, Tokyo 113-0033, Japan. E-mail: kmiya@mol.f.u-tokyo.ac.jp, uchiyama@mol.f.u-tokyo.ac.jp*
[c] *Research Initiative for Supra-Materials (RISM), Shinshu University, 3-15-1 Tokita, Ueda, 386-8567, Japan*

† Electronic supplementary information (ESI) available. See DOI: https://doi.org/10.1039/d2cp01214f

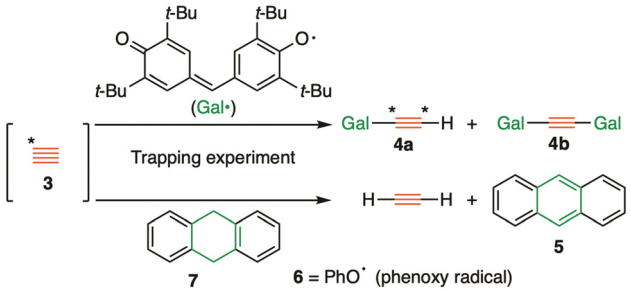

Fig. 2 Trapping experiments used for inferring the existence of singlet free C_2.

temperature production of C_2 seemed unlikely. A follow up analysis[7] explored the possibility that bimolecular reactions between **2** and the traps (path 2, Fig. 1), or between **2** and itself to give ultimately polymeric carbon (path 3, Fig. 1), might provide alternative mechanistic routes to the observed products and which would also rationalise the ^{13}C scrambling, whilst avoiding liberation of free C_2. Here this study is extended to computing the bimolecular transition states and unimolecular fragmentation energies using a variety of different leaving groups X, in order to establish how the energetics of the mechanistic paths shown in Fig. 1 respond to the nature of the nucleofuge group X (Fig. 1). As a result of these studies we felt in appropriate to then suggest that the original experiments be repeated with a new selection of leaving groups X. Accordingly, the experimental response of the putative C_2 precursors **1a–d** with different nucleofuges (**1a:** X = iodo, **1b:** λ^3-iodanyl, **1c:** pyridinio, and **1d:** dibenzosulfonio groups) to trapping experiments was undertaken to establish the scope of this method for generating putative **3**.

Computational details

The CHAMP portal[8] was used as an electronic notebook for managing the project, enabled with one-click FAIR data publishing to the Imperial College data repository.[9] To study the energetics and mechanism of these reactions, a calibrated procedure was selected as used previously;[6] ωB97XD[10]/Def2-TZVPPD[11]/SCRF[12] = dichloromethane solvent.[13] The calibration involved comparison of computed energies for C_2[14] against the reaction sequence shown in Scheme 1, the energies of which are directly derived from experimental measurements.[15] The CCSD(T) couple-cluster method[16] emerged as closely matching the experimental results for the thermochemistry of formation of C_2. A variety of DFT-based methods were tested and all predicted the energy of the highly correlated C_2 species to be significantly too high; if corrected by 28 kcal mol^{-1}, the ωB97XD DFT method can be brought into congruence with both experiment and the CCSD(T) method. This correction is applied only to reactions involving C_2. For the substitution reactions described below, which do not involve this species, the uncorrected ωB97XD and the CCSD(T) methods agreed[7,14] to within 1.5 kcal mol^{-1} for a model system X = MeI (larger groups are not computationally viable using the CCSD(T) method, where computation times of >10 years were estimated for the groups X described below). Further cancellation of error might be expected for a range of reactions differing only in the nature of group X (Fig. 1). All located transition states have one negative force constant with the correct vectors, which can be inspected as 3D animated models using a FAIR-enabled version of Table 1.[17]

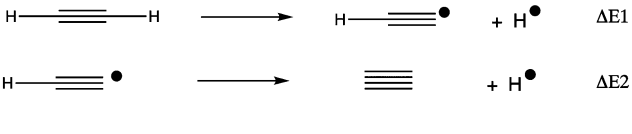

Scheme 1 Calibration reactions for thermochemistry.

Experimental details

Substrates

Iodoalkyne **1a**, alkynyl(aryl)-λ^3-iodane **1b**, *N*-alkynylpyridinium salt **1c**, and *S*-alkynylsulfonium salt **1d** were prepared according to the reported procedures (S1–S4, ESI†). All of these starting materials used were greater than 99% purity, which was confirmed by ^1H NMR. ^1H NMR spectra of **1a–d** are shown in the ESI† (Section 4, copies of ^1H NMR spectra and GCMS chart). Tetrabutylammonium fluoride trihydrate (≥98%),

Table 1 Calculated ωB97XD/Def2-TZVPPD/SCRF = DCM Free energies for reactions of 2[a]

2, X=	$\Delta\Delta G_{(3+X)-2}$[b]	$\Delta\Delta G^{\ddagger}_{TS1,1}$[c]	$\Delta\Delta G^{\ddagger}_{TS1,2}$[c]	ΔΔ*G*, unimolecular *vs.* bimolecular[d]
2Pyridinium	83.7	30.1	27.9	55.8
Pyridinium + **6**[e]	83.7	23.8	24.8	59.9
Pyridinium + **7**[f]	83.7	47.8	27.9	55.8
$2Me_3P$	117.6	45.7	34.5	83.1
$2Me_2O$	42.3	23.7	24.6	18.6
$2Me_2S$	79.6	34.3	27.2	52.4
Me_2S + **6**	79.6	27.4	24.4	55.2
Me_2S + **7**	79.6	45.6	28.0	51.6
2Dibenzothiophenium	64.0	32.8	26.9	37.1
Dibenzothiophenium + **6**	64.0	27.4	25.0	39.0
$2Me_2Se$	77.1	33.2	28.1	49.1
$2Me_2Te$	82.7	35.4	26.5	56.2
2MeF	−2.4	12.9	14.9	−15.3
2MeCl	32.1	22.7	21.0	11.1
2MeBr	35.6	22.0	19.4	16.2
2MeI	46.0	24.5	21.4	24.6
2PhI	43.6	23.1	19.6	24.0
PhI + **6**	43.6	19.6	19.6	24.0
$2MeF_2I$	36.3	20.3	12.5	23.8
MeF_2I + **6**	36.3	26.3	23.2	13.1

[a] Calculations at the ωB97XD/Def2-TZVPPD/SCRF = dichloromethane level, data repository collection DOI: 10.14469/hpc/8168 for full details of calculation. [b] ΔΔ*G* for the reaction **2** → (**3** + **X**) in kcal mol^{-1}, corrected by −28.0 kcal mol^{-1} for estimated error in the calculated Δ*G* for C_2 at this level. [c] $\Delta\Delta G_{298}$ transition state activation energies in Hartree for $TS_{1,1}$ or $TS_{1,2}$ the substitution step; for a standard state of 0.044M (1 atm). [d] ΔΔ*G* (kcal mol^{-1}) for unimolecular fragmentation of $\Delta G_{(3+X)-2}$ − the lower of $\Delta G_{TS1,1}$ or $\Delta G_{TS1,2}$.

9,10-dihydroanthracene (>98.0%(GC)), galvinoxyl free radical, iodobenzene (>99.0%(GC)), 4-phenylpyridine (>98.0%(GC)), and dibenzothiophene (>98.0%(GC)) were purchased from Tokyo Kasei Co. The purity of these reagents (except for galvinoxyl free radical) was also confirmed by ^{1}H NMR (NMR spectra are shown in Section 4, copies of ^{1}H NMR spectra and GCMS chart) prior to use. The purity of galvinoxyl free radical was confirmed by GC/GCMS and was determined to be >99%. Dichloromethane (>99.5% by gas chromatography) was purchased from Kanto Chemical Co., Inc., degassed by purging with argon, and dried with a solvent purification system containing a one-meter column of activated alumina. All trapping reactions were carried out either in a two-necked flask or connected flasks under an argon atmosphere.

General procedure

To a stirred solution of C_2-precursor **1** (0.065 mmol) and trapping agent (50 equivalent for 9,10-dihydroanthracene and 1.2 equivalent for galvinoxyl radical) in dichloromethane (1.3 mL), tetrabutylammonium fluoride trihydrate (1.2 equivalent) was added in one portion at −78 °C and the solution was gradually warmed to room temperature for 3–72 h (disappearance of starting material was monitored by ^{1}H NMR, except for **1a**). After concentration of the reaction mixture under a reduced pressure, the resulting residue was then analyzed by ^{1}H NMR (ethyl acetate as an internal standard) and atmospheric pressure chemical ionization mass spectrometry (APCIMS). For the trapping reaction with galvinoxyl radical, excess 1,4-cyclohexadiene was added (in order to quench any remaining galvinoxyl radical) prior to ^{1}H NMR measurement. The formation of acetylene was confirmed by GCMS with a PLOT column (Rt-U-Bond, 0.25 mm × 30 m, 30 °C) or silver nitrate testing.

Solvent-free connected flask experiment

S-(Trimethylsilylethynyl)dibenzothiophenium salt **1d** (33 mg, 0.077 mmol) and cesium fluoride (35.0 mg, 0.231 mmol) was placed in one of a pair of connected flasks (Flask A), and galvinoxyl radical (97 mg, 0.231 mmol) was placed in the other flask (Flask B). The reaction mixture in Flask A was vigorously stirred at room temperature for 48 hours under argon. The contents of Flask B were directly analyzed by APCIMS. The contents of Flask A were analyzed by ^{1}H NMR (ethyl acetate was an internal standard).

Results and discussion

There are two basic mechanisms for the reaction of the zwitterionic species **2**, namely unimolecular fragmentation to give **3** (free C_2) followed by bimolecular trapping of this species (Fig. 1, path 1) or immediate bimolecular reactions involving no free C_2 (paths 2 and 3). The presence of the species **2** (X = IPh) has been confirmed during the fluorolysis of alkynyl(aryl)-λ^3-iodane with Bu_4NF in dichloromethane and was stable below −30 °C.[3] One potential strategy for differentiating between these mechanistic pathways would be to vary the nature of the group X. The leaving group ability of X would be expected to impact directly upon the unimolecular fragmentation path 1, whereas its effect might be attenuated for the bimolecular trapping paths 2 or 3 (Fig. 1). To explore if this hypothesis is correct, the energetics for a variety of new leaving groups X were obtained computationally using density functional theory, with the results collected in Table 1.[17] This shows the energetics of bimolecular dimerization of species **2** (path 3) as well as reaction of **2** with either dihydroanthracene or a phenoxy radical model as trapping agents (path 2). The calculated ωB97XD DFT free energy of the two-stage unimolecular dissociation path 1 needs correction for the exceptional error in the calculated energy of **3** itself, as described previously.[6,14,15] The difference in free energy between the dissociation path 1 and the transition states leading to bimolecular reaction *via* either 1,1 or 1,2 substitution[7] (paths 2 or 3) is shown in the last column of the table. The effect the nature of the leaving group X has on this difference will now be discussed.

We start by noting that for the substituents X = Me_3P through to MeF, the calculated free energy of unimolecular dissociation of **2** to give X and **3** (C_2) spans $\Delta\Delta G$ = 117.6 to −2.4 kcal mol^{-1}. Of these, only values < ~35 kcal mol^{-1} would be considered as thermally accessible below ~313 K. In contrast, the activation barriers for direct bimolecular reactions of **2** over this span of substituents range from $\Delta\Delta G^{\ddagger}$ 34.5 to 12.5 kcal mol^{-1}, a very much smaller span for which the entire range is potentially thermally accessible. The last column in Table 1 indicates the difference in free energy between the unimolecular dissociation path 1 resulting in the formation of **3** from **2** and the lowest energy of the two bimolecular paths 2 and 3 for reaction of **2** involving either 1,1- or 1,2-substitution.[7] We note that the relative free energy of path 1 in this column should be increased by a further ~10 kcal mol^{-1} to reflect the entropic penalty for the bimolecular reaction between **3** and trap, with the thermal barrier for this reaction expected to be very small or even zero.[7] For leaving groups such as X = pyridinium, the difference between the paths is so large that one might confidently state that only bimolecular paths 2 and 3 are viable. There is only one substituent for which unimolecular dissociation is actually predicted to be more favourable than the bimolecular mode, and that is for X = MeF, which is not a realistic group for synthetic testing. The activation free energy of the bimolecular route for *e.g.* X = dibenzothiophenium is ~25 kcal mol^{-1}, which can be considered as falling into a thermally accessible range. This example and X = pyridinium are the ones that were selected for experimental testing, by virtue of their synthetic accessibility.

Following this theoretical evaluation, we turned to an experimental protocol for evaluating the ability of the C_2 precursors **2**, as potentially generated from the starting materials **1a–d** representing different nucleofuges (X = iodo, λ^3-iodanyl, pyridinio, and sulfonio groups respectively), to be trapped using our previous radical trapping protocol.[3] Firstly, the attempted reaction of (trimethylsilyl)iodoacetylene (**1a**, X = iodo) with a fluoride ion source (Bu_4NF) in the presence

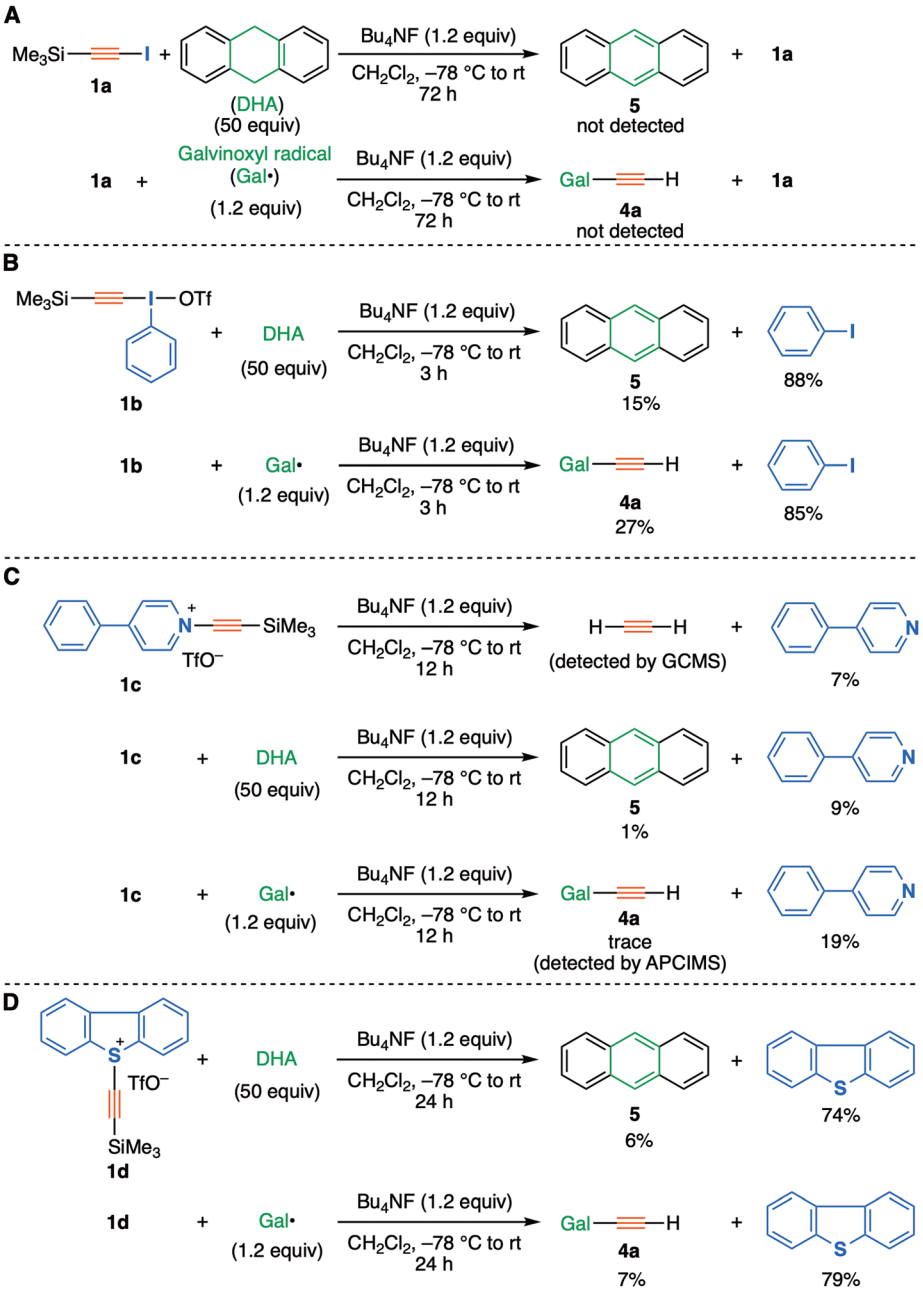

Fig. 3 Trapping experiments with (A) iodoacetylene **1a**, (B) alkynyl-λ^3-iodanes **1b**, (C) 4-phenyl-pyridinium salt **1c**, (D) dibenzosulfonium salt **1d**.

of galvinoxyl radical or 9,10-dihydroanthracene was investigated (Fig. 3A), but no distinct evidence was obtained for the formation of radical-trapped products (ethynylated galvinoxyl **4a**, anthracene **5**), nor was acetylene detected and alkyne **1a** was recovered exclusively. In sharp contrast, as expected, alkynyl-λ^3-iodane **1b** (X = λ^3-iodanyl), which has *ca.* 10^{12} times greater nucleofuge capability (-I(Ph)X) than an iodo group,[18] led to good yields of trapped products **4a** or **5** under similar reaction conditions. This confirms the importance of the nucleofuge in this transformation (Fig. 3B).

Significantly, the theoretically evaluated pyridinium-type precursor **1c** (X = 4-phenylpyridinium triflate) was also found to serve as a precursor. Thus, in the presence/absence of trapping agents, not only acetylene gas but also radical-trapped products **4a** or **5** were detected/obtained in low yields, being accompanied by the formation of 4-phenylpyridine (Fig. 3C). Similar to our previous report, the formation of di(galvinoxy)acetylene **4b** was not observed in solution, probably due to the rapid hydrogen abstraction of transient ethynyl radical from the solvent, dichloromethane.[3,19] All of these experimental results suggest that the *in situ* generation of the zwitterionic species **2** could act as a C_2 synthon, even with much a much weaker leaving group such as 4-phenylpyridine. However this result does not distinguish between unimolecular

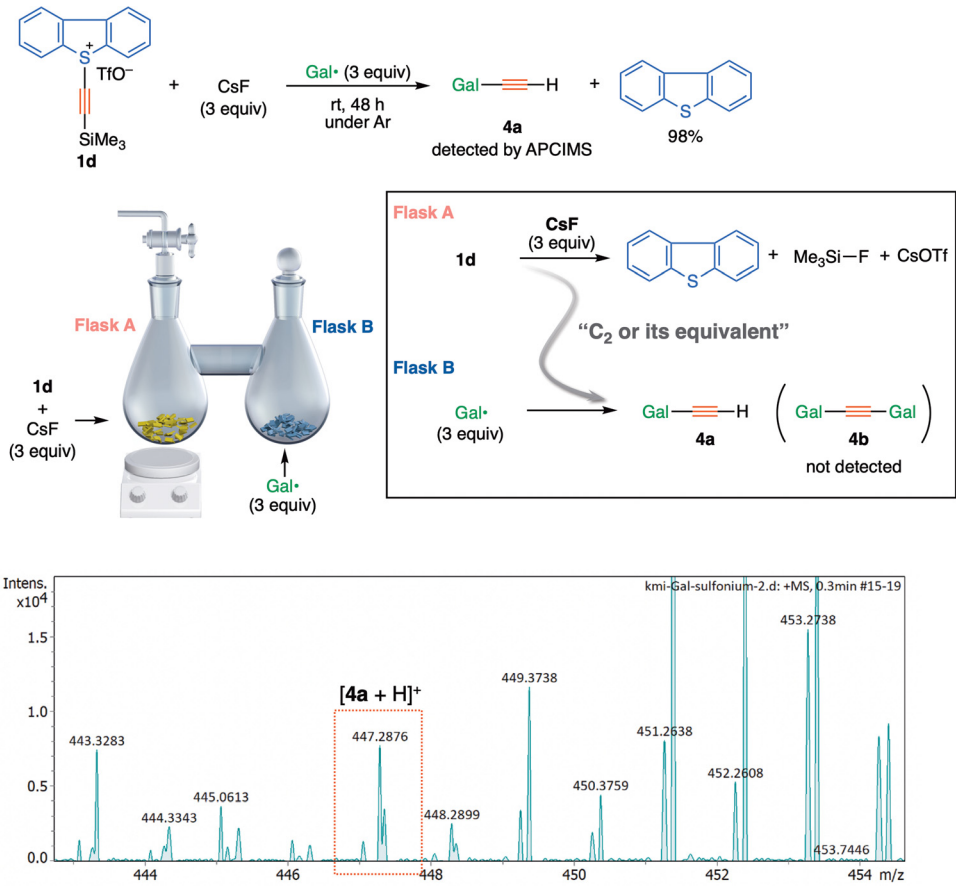

Fig. 4 Solvent-free connected flask experiment using sulfonium salt **1d**-CsF and galvinoxyl radical. (A) Reaction conditions. (B) Details of reaction equipment. (C) Atmospheric-pressure chemical ionisation (APCIMS) spectrum of the contents in a flask B.

and bimolecular trapping mechanisms (path 1 *vs.* path 2). The activation free energy for path 2 bimolecular trapping is predicted to be within a thermally accessible range, whereas the energy for path 1 is computed to be 60 + ~10 = ~70 kcal mol^{-1} higher than that for path 2 (Table 1).

Use of the dibenzothiophenium precursor **1d**, which bears a more potent nucleofuge than pyridine, has provided further evidence in the form of higher yields of trapped products **4a** and **5** as obtained under similar conditions (Fig. 3D). The computed path 2 bimolecular free energy barriers for this substituent and the pyridinium-type substrate were similar (Table 1). Based on these two trapping experiments, we consider that the rate of desilylation yielding intermediate **2** as well as the following processes has a relatively modest dependency on both the electron withdrawing- and the leaving group ability of X in the precursors **1**. This is more congruent with the predicted behaviour of path 2 rather than of path 1, for which a much higher dependency on X is predicted.

Significantly however, the solid-state solvent-free connected flask experiment using sulfonium **1d** also afforded a trapped product **4a**, although to a small extent (Fig. 4). The presence of **4a** in a separated flask (Flask B) suggests that the evolution of a volatile species, presumed to be **3**, would occur in Flask A, which is consistent with the previous results obtained with alkynyl-λ^3-iodane **1b** and **1b**-^{13}C (counter ion: BF_4^-).[3,19] The absence of di(galvinoxyl)acetylene **4b** in Flask B might reflect the poorer ability of **1d** (X= dibenzothiophenium) to act as a precursor of **3**, compared with **1b** (X = λ^3-iodanyl) under the reaction conditions.

At this stage therefore, we cannot explain the discrepancy between the (solid-state solvent-free connected flask) experimental results and theoretical estimations of the energy required to liberate a free C_2 species. An alternative mechanism might be necessary to solve the conundrum.

Conclusions

The single-flask solution phase experiments indicating trapping using two different precursors **2** (X = pyridinium and dibenzothiophenium) are consistent with a bimolecular mechanism (path 2) involving no liberation of free **3**. The theoretical free energies of the unimolecular path 1 for X = dibenzothiophenium and particularly for pyridinium are so much higher than it seems less likely that this mechanism could be followed. A mystery remains however for the connected flask trapping experiment, which suggest that the precursor with the good nucleofuge **1d** can produce an

argon-borne intermediate that results in transfer to flask B and then apparent trapping of C_2 (**3**). This seemingly indicates that path 1 is followed under these conditions, despite the contra-indications from the theoretical evaluation. More experiments to further confirm the identity of this gas-borne intermediate and perchance provide insight into the experimental/theoretical dichotomy are needed.

Data availability

All relevant FAIR (Findable, Accessible, Interoperable, Reusable) datasets are available from a data repository *via* the master collection DOI: 10.14469/hpc/8168 and datasets cited therein.

Author contributions

H. S. Rzepa performed the calculations, M. Arita, K. Miyamoto and M. Uchiyama performed the experiments and all authors contributed to writing the text.

Conflicts of interest

The authors declare no conflicts of interest.

Notes and references

1 T. W. Schmidt, *Acc. Chem. Res.*, 2021, **54**, 481–489, DOI: 10.1021/acs.accounts.0c00703.
2 S. Shaik, H. S. Rzepa and R. Hoffmann, *Angew. Chem.*, 2013, **52**, 3020–3033.
3 K. Miyamoto, S. Narita, Y. Masumoto, T. Hashishin, M. Kimura, M. Ochiai and M. Uchiyama, *ChemRxiv*, 2019, preprint, DOI: 10.26434/chemrxiv.8009633.
4 K. Miyamoto, S. Narita, Y. Masumoto, T. Hashishin, T. Osawa, M. Kimura, M. Ochiai and M. Uchiyama, *Nat. Commun*, 2020, **11**, 2134, DOI: 10.1038/s41467-020-16025-x.
5 H. S. Rzepa, *ChemRxiv*, 2020, preprint, DOI: 10.26434/chemrxiv.12237980.
6 H. S. Rzepa, *Nat. Commun.*, 2021, **12**, 1241, DOI: 10.1038/s41467-021-21433-8.
7 H. S. Rzepa, *Phys. Chem. Chem. Phys.*, 2021, **23**, 12630–12636, DOI: 10.1039/D1CP02056K.
8 M. J. Harvey, N. J. Mason and H. S. Rzepa, *J. Chem. Inf. Model.*, 2014, **54**, 2627–2635, DOI: 10.1021/ci500302p; C. Cave-Ayland, M. J. Bearpark, C. Romain and H. S. Rzepa, *J. Open Source Soft.*, 2022, **7**, 3824, DOI: 10.21105/joss.03824.
9 M. J. Harvey, A. McLean and H. S. Rzepa, *J. Cheminform.*, 2017, **9**, 4, DOI: 10.1186/s13321-017-0190-6.
10 J.-D. Chai and M. Head-Gordon, *Phys. Chem. Chem. Phys.*, 2008, **10**, 6615–6620, DOI: 10.1039/B810189B.
11 B. P. Pritchard, D. Altarawy, B. Didier, T. D. Gibson and T. L. Windus, *J. Chem. Inf. Model.*, 2019, **59**, 4814–4820, DOI: 10.1021/acs.jcim.9b00725.
12 M. Cossi, N. Rega, G. Scalmani and V. Barone, *J. Comp. Chem.*, 2003, **24**, 669–681, DOI: 10.1002/jcc.10189.
13 M. J. Frisch, G. W. Trucks, H. B. Schlegel, G. E. Scuseria, M. A. Robb, J. R. Cheeseman, G. Scalmani, V. Barone, G. A. Petersson, H. Nakatsuji, X. Li, M. Caricato, A. V. Marenich, J. Bloino, B. G. Janesko, R. Gomperts, B. Mennucci, H. P. Hratchian, J. V. Ortiz, A. F. Izmaylov, J. L. Sonnenberg, D. Williams-Young, F. Ding, F. Lipparini, F. Egidi, J. Goings, B. Peng, A. Petrone, T. Henderson, D. Ranasinghe, V. G. Zakrzewski, J. Gao, N. Rega, G. Zheng, W. Liang, M. Hada, M. Ehara, K. Toyota, R. Fukuda, J. Hasegawa, M. Ishida, T. Nakajima, Y. Honda, O. Kitao, H. Nakai, T. Vreven, K. Throssell, J. A. Montgomery, Jr., J. E. Peralta, F. Ogliaro, M. J. Bearpark, J. J. Heyd, E. N. Brothers, K. N. Kudin, V. N. Staroverov, T. A. Keith, R. Kobayashi, J. Normand, K. Raghavachari, A. P. Rendell, J. C. Burant, S. S. Iyengar, J. Tomasi, M. Cossi, J. M. Millam, M. Klene, C. Adamo, R. Cammi, J. W. Ochterski, R. L. Martin, K. Morokuma, O. Farkas, J. B. Foresman and D. J. Fox, *Gaussian 16, Revision C.01*, Gaussian, Inc., Wallingford CT, 2016.
14 H. S. Rzepa, Imperial College Research Data Repository, 2021, DOI: 10.14469/hpc/7721.
15 D. Danovich, P. C. Hiberty, W. Wu, H. S. Rzepa and S. Shaik, *Chem. Euro. J.*, 2014, **20**, 6220–6232, DOI: 10.1002/chem.201400356, and Table 2 therein.
16 G. D. Purvis III and R. J. Bartlett, *J. Chem. Phys.*, 1982, **76**, 1910–1918, DOI: 10.1063/1.443164.
17 H. S. Rzepa, Imperial College Research Data Repository, 2021, DOI: 10.14469/hpc/8280 and the master collection at DOI: 10.14469/hpc/8168.
18 T. Okuyama, T. Takino, T. Sueda and M. Ochiai, *J. Am. Chem. Soc.*, 1995, **117**, 3360–3367, DOI: 10.1021/ja00117a006.
19 K. Miyamoto, S. Narita, Y. Masumoto, T. Hashishin, T. Osawa, M. Kimura, M. Ochiai and M. Uchiyama, *Nat. Commun.*, 2021, **12**, 1245, DOI: 10.1038/s41467-021-21439-2.